Cell Reports, Volume *42*

Supplemental information

Neuroendocrine lineage commitment of small cell lung cancers can be leveraged into p53-independent non-cytotoxic therapy

Sudipta Biswas, Kai Kang, Kwok Peng Ng, Tomas Radivoyevitch, Kurt Schalper, Hua Zhang, Daniel J. Lindner, Anish Thomas, David MacPherson, Brian Gastman, David S. Schrump, Kwok-Kin Wong, Vamsidhar Velcheti, and Yogen Saunthararajah

SUPPLEMENTARY MATERIAL

Neuroendocrine lineage commitment of small cell lung cancers can be leveraged into p53-independent non-cytotoxic therapy

Sudipta Biswas[1], Kai Kang[1], Kwok Peng Ng[1], Tomas Radivoyevitch[2], Kurt Schalper[3], Hua Zhang[4], Daniel J. Lindner[1], Anish Thomas[5], David MacPherson[6], Brian Gastman[7], David S. Schrump[8], Kwok-Kin Wong[4], Vamsidhar Velcheti[4], Yogen Saunthararajah[1,9]

Table S1 (related to Figures 1 and S1)(Excel file). Expression of ASCL1-target, MYC-target, and pulmonary neuroendocrine-lineage genes in normal pulmonary neuroendocrine cells and SCLC cell lines.

Table S2 (related to Figures 1 and S1) (Excel file). CpG sites and methylation values at ASCL1-target, MYC-target and pulmonary neuroendocrine-lineage genes in embryonic stem cells and SCLC cell lines.

Table S3 (related to Figures 1 and S1) (Excel file). CpG Methylation at NE-Lineage Genes

Table S4 (related to Figure S2) (Excel file): Neuroendocrine genes analyzed

Table S5 (related to Figure 3D and Figure S2) (Excel file): RNA-seq Normalized Counts H146 F1339 Veh vs Dec.

Table S6 (Excel file): (primer sequences)

9 supplementary figures

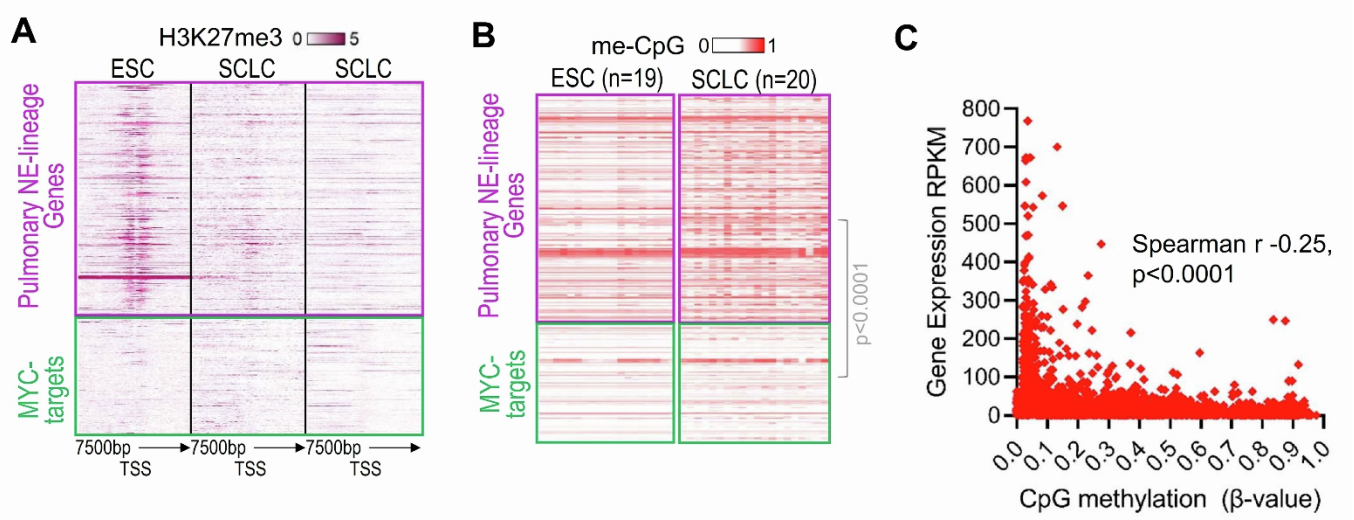

Figure S1 (related to Figure 1). Neuroendocrine genes, but not MYC-target genes, are enriched for H3K27me3 and me-CpG epigenetic repression marks in embryonic stem cells (ESC); SCLC cells erase H3K27me3 but not me-CpG from neuroendocrine genes. A) H3K27me3 is enriched at pulmonary neuroendocrine-lineage genes but not MYC-target genes at baseline in ESC and erased in SCLC cells. ChIP-seq H1 ESC cells (GSM733748 Encode) and H69 SCLC cells and H1963 SCLC cells (GSM5133639, GSM5005200[1]). **B) me-CpG is enriched at pulmonary neuroendocrine-lineage genes over MYC-targets at baseline in ESC, a pattern that is preserved into SCLC cells.** Genes specific to neuroendocrine-lineage (Table S3) were identified from an atlas of single-cell gene expression by RNA-sequencing in normal human lung and a murine model of neuroendocrine-lineage differentiation[2,3]. Mann-Whitney test, 2-sided. DNA methylation (β-values) at CpG in CpG-islands associated with the indicated genes in 450K Illumina array annotation (ESC cells GSE31848[4]; SCLC cell lines GSE66295[5]). Table S3. **C) Negative correlation between me-CpG and gene expression at neuroendocrine-lineage genes in SCLC cells.** The expression of these genes measured by RNA-sequencing (RPKM, Cancer Cell Line Encyclopedia) was correlated with average methylation levels at CpG islands linked to the gene (β-values, 450K Illumina array, GSE66295[5]) in individual SCLC cell lines (n=17). P-value, 2-sided.

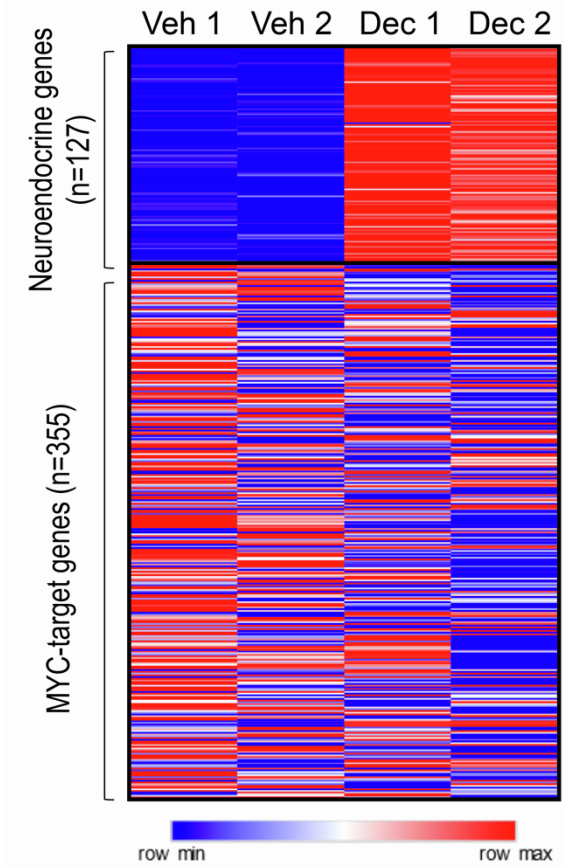

Figure S2 (related to Figure 2). Neuroendocrine lineage genes were upregulated by decitabine treatment of H146 cells. Small cell lung cancer cells H146 were treated with vehicle control DMSO or decitabine (Dec) 0.5 μM for 96 hours (2 biological replicates), then cells were harvested for gene expression analysis by RNA-sequencing. Read counts were normalized (size factor normalization) then differentially expressed genes between vehicle and Dec treatment identified using the DESeq2 tool: the Wald test was used to generate p-values and log2 fold changes, and genes with an adjusted p-value < 0.05 and absolute log2 fold change > 1 were called as differentially expressed genes. Of 1146 genes that were significantly upregulated by Dec treatment, 127 were apriori neuroendocrine genes (Table S4), while none were MYC-target genes. The normalized counts of MYC-target genes (n=355 identified by chromatin immunoprecipitation as cited in text) are included in the figure by way of internal control.

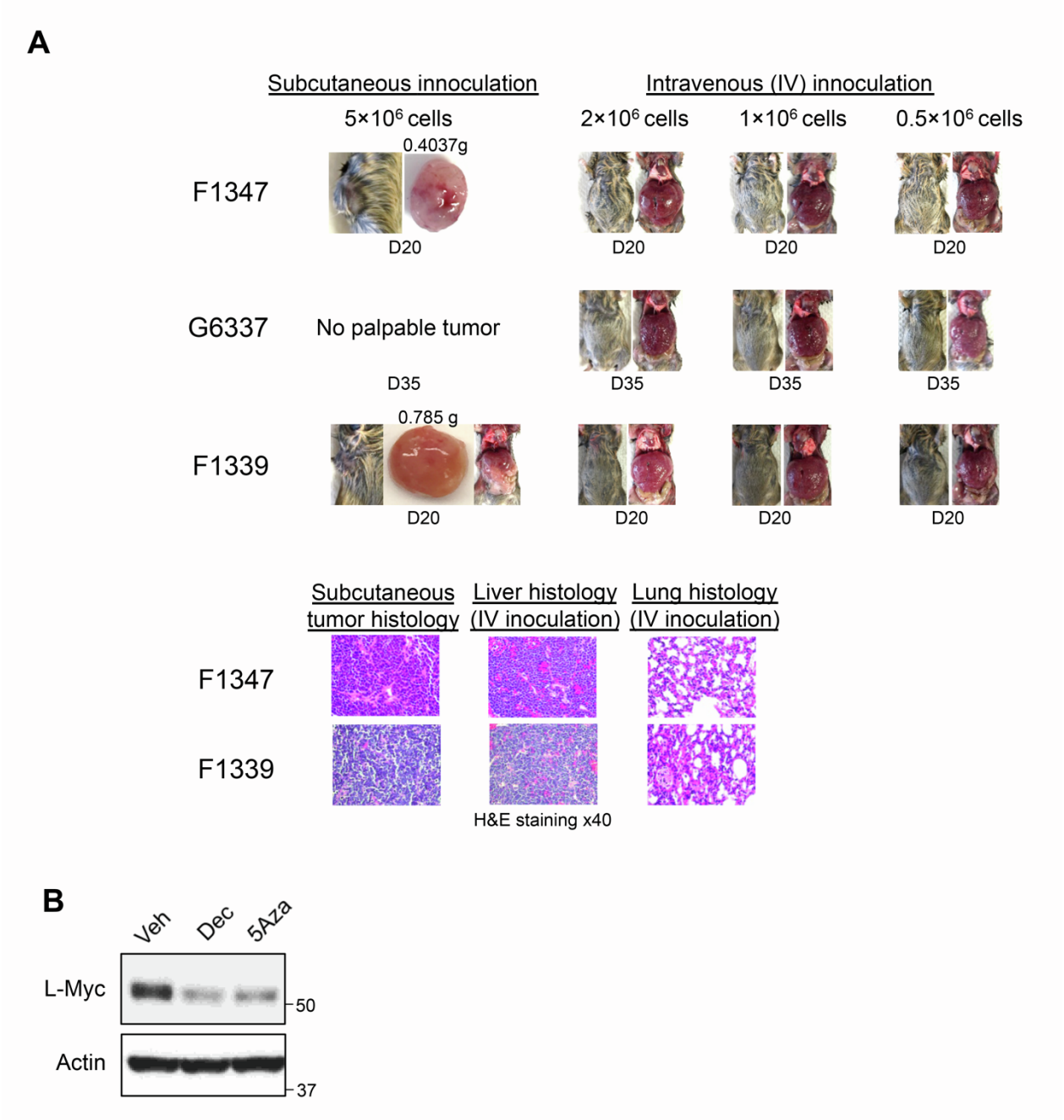

Figure S3 (related to Figure 3). A. To evaluate efficacy of DNMT1-targeting to treat SCLC in vivo, alone or in combination with ICI, we employed a syngeneic, immunocompetent, genetically engineered mouse model of SCLC that recapitulates key genetic characteristics of human SCLC of *RB* and *TP53* inactivation, established in vivo by intra-tracheal instillation of Adeno-CMV-Cre in $Rb^{lox}/p53^{lox}$ mice, used also by others to answer therapy questions in SCLC. We evaluated several iterations of this model to identify SCLC cells that also captured aggressiveness of metastatic spread of human SCLC after subcutaneous innoculation, with metastases to sites such as the liver, the most frequent site of spread in extensive stage disease. Images show gross and histological appearances of subcutaneous tumor and of the liver, and histological appearance of the lungs, after subcutaneous or intravenous inoculation of separately generated SCLC cells. The F1339 model was selected since it demonstrated aggressive in vivo spread and also grew in vitro, enabling parallel in vitro experiments. **B. Dec and 5Aza treatment decreased L-Myc expression.** Murine SCLC, F1339 cells were treated with DMSO vehicle control, decitabine 0.5 μM or 5-azacytidine 5 μM. L-Myc expression was measured by Western blot analysis. Actin used as control.

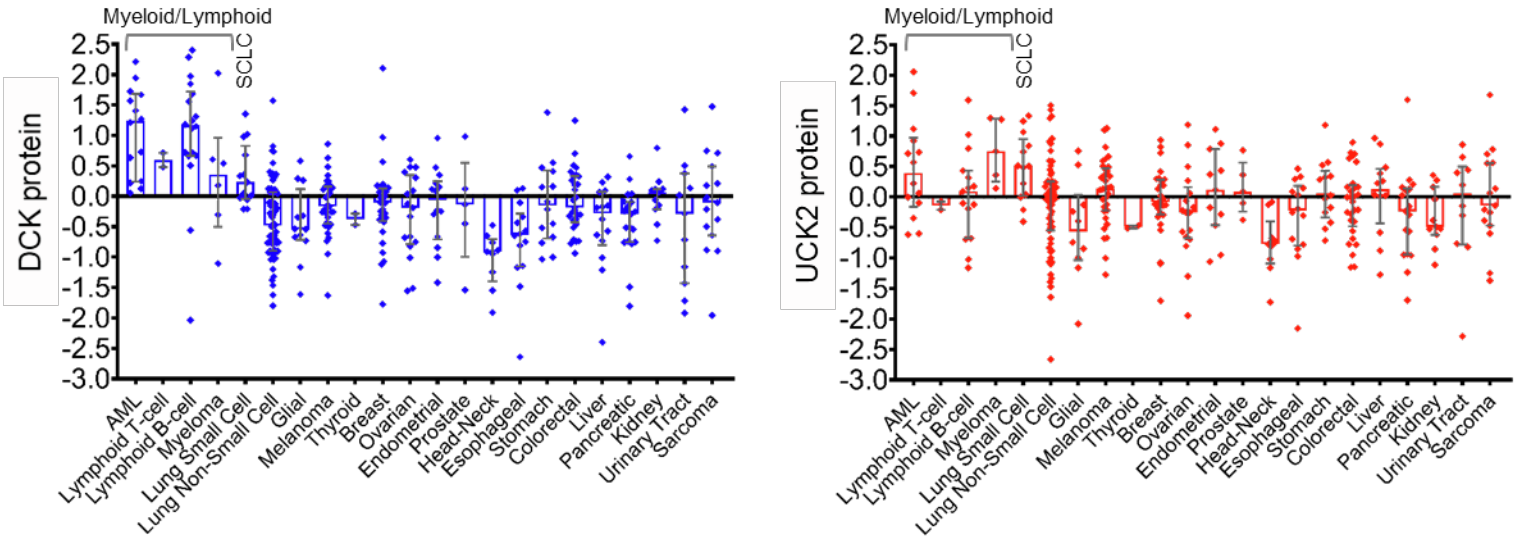

Figure S4 (related to figure 3). SCLCs express DCK and UCK2 protein at levels comparable to myeloid and lymphoid cancers routinely treated with DCK- and UCK2-dependent pro-drugs. Quantitative protein profiling by mass-spectrometry, values are protein-level probability estimates as described in Cancer Cell Line Encyclopedia (CCLE) public data[6]. Median±IQR.

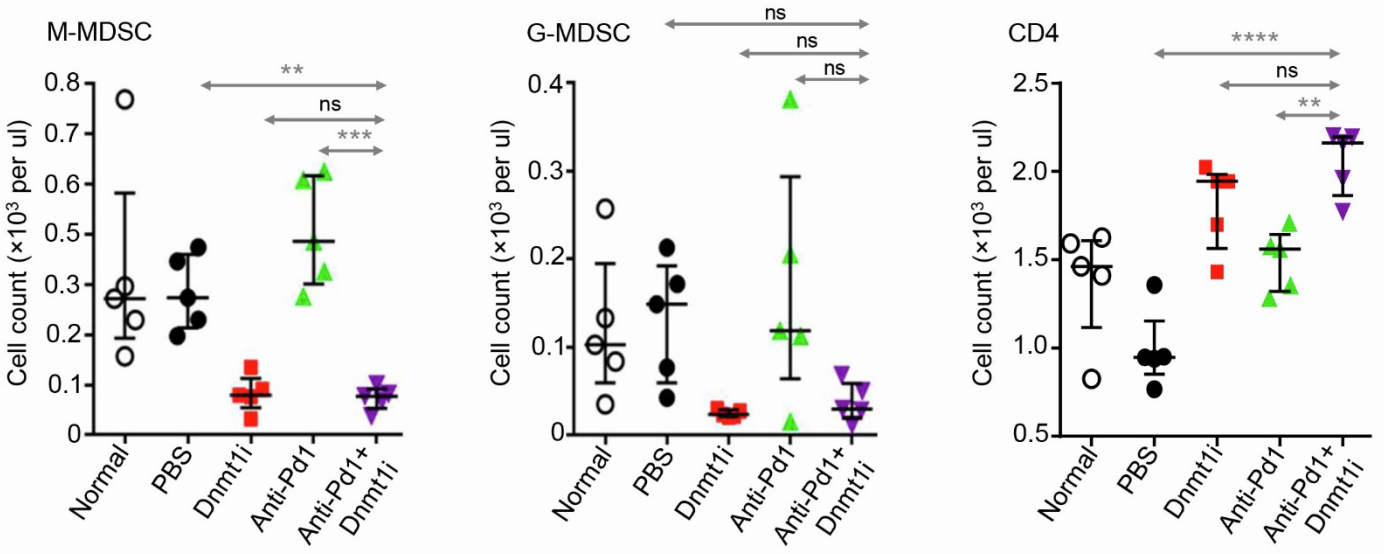

Figure S5 (related to Figure 4). **Dnmt1-targeting treatment (Dnmt1i), ICI and combination Dnmt1i + ICI similarly decreased peripheral blood (PB) granulocytic and monocytic myeloid-derived suppressor cells (G-MDSC and M-MDSC), while peripheral blood CD4+ T-cells were significantly and similarly increased**. B6/129 SF1 mice were inoculated via tail vein with F1339-luc lung cancer cells (0.3×10^6 cells/mouse). After documentation of tumor invasion by live-imaging, mice (n = 5/group) were randomized to PBS, THU-Dec/5Aza, anti-Pd1 or combination anti-Pd1+THU-Dec/5Aza. Bar and whiskers = Median ± IQR. **p < 0.01; ***p < 0.001; ****p < 0.0001. ns: p > 0.05. 2-sided Mann-Whitney test.

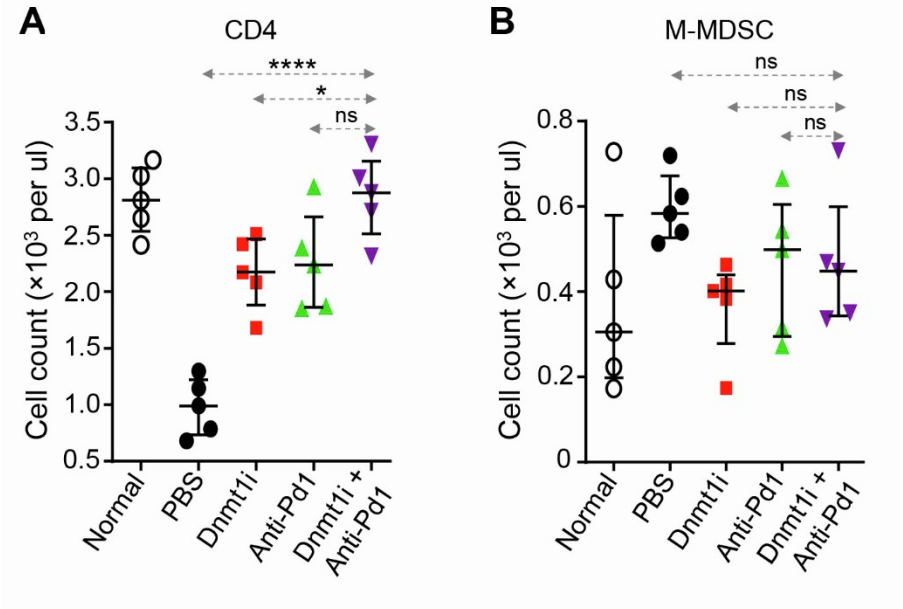

Figure S6 (related to Figure 5). A non-cytotoxic Dnmt1-targeting regimen (Dnmt1i) was active against p53-null, chemorefractory SCLC in vivo. B6/129 SF1 mice were tail-vein inoculated with F1339-luc SCLC cells (0.3×10^6 cells/mouse). After documentation of tumor invasion by live-imaging, mice (n = 5/group) were randomized to PBS, Dnmt1-targeting treatment with THU/Dec/5Aza, anti-Pd1 or Dnmt1-targeting + anti-Pd1. Bar and whiskers = Median±IQR. *$p < 0.05$; ****$p < 0.0001$; ns: $p > 0.05$. 2-sided Mann-Whitney test. **A) Peripheral blood CD4+ T-cells.** Measured by Hemavet and flow cytometry at time-of-euthanasia. **B) Peripheral blood monocyte myeloid-derived suppressor cells (M-MDSC).** Measured by Hemavet and flow cytometry at time-of-euthanasia.

.

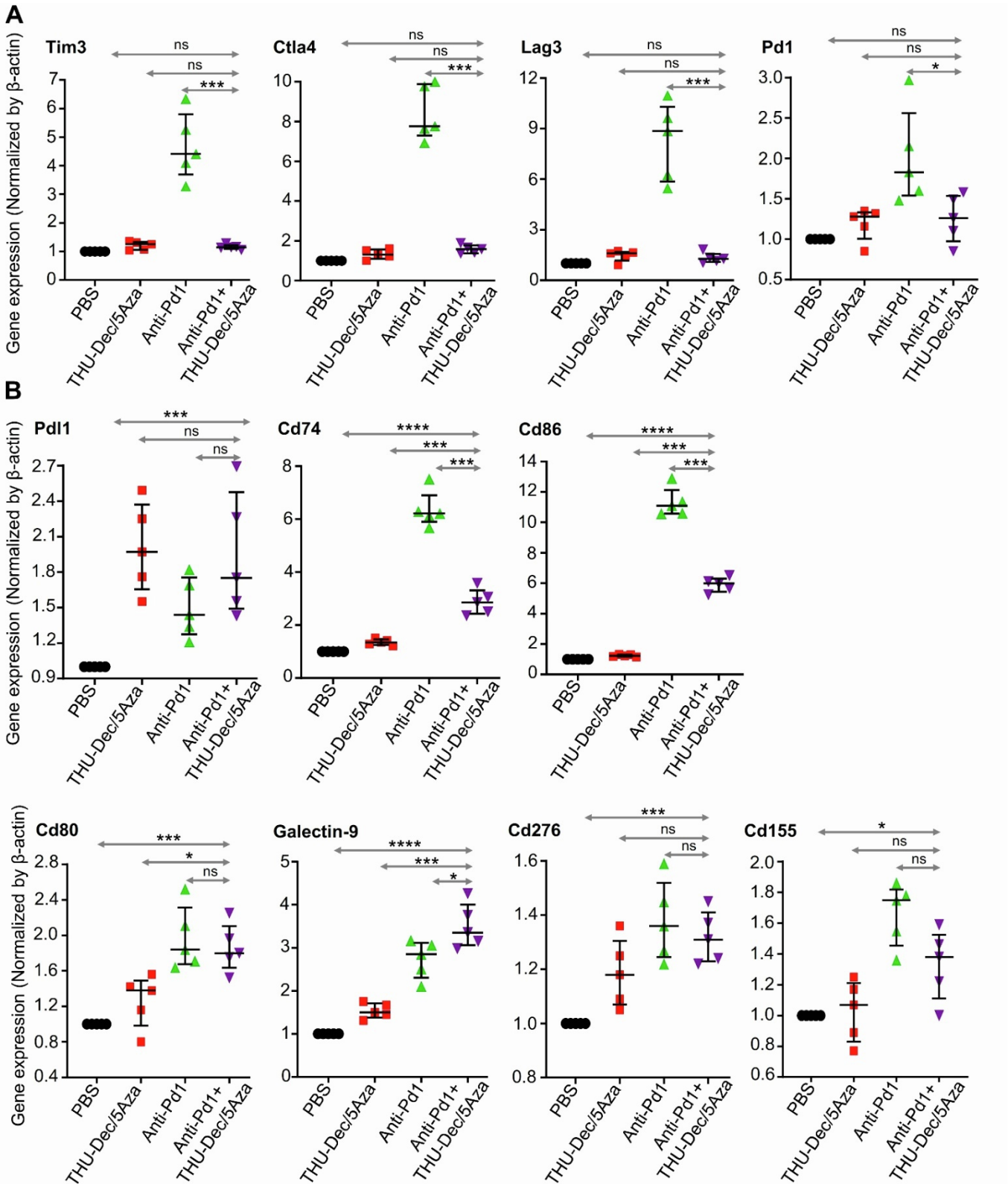

Figure S7 (supplement to Figure 5). SCLC tumors in anti-Pd1 treated mice demonstrated upregulation of several immune checkpoints other than Pd1/Pd-l1. B6/129 SF1 mice were tail-vein inoculated with F1339-luc SCLC cells (0.3×10^6cells/mouse). After documentation of tumor engraftment by live-imaging, mice (n = 5/group) were randomized to PBS, Dnmt1-targeting with THU-Dec/5Aza, anti-PD1 or combination Dnmt1-targeting + anti-PD1. Bar and whiskers = median±IQR. *$p < 0.05$; ***$p < 0.001$; ****$p < 0.0001$; ns: $p > 0.05$. 2-sided Mann-Whitney test. **A) Immune-checkpoint expression in TILs.** TILs from 5 individual mice per group (magnetically selected for $CD8^+$ expression). **B) Immune-checkpoint expression in SCLC tumor tissue after 14 days of treatment.** Tumor tissue from 5 individual mice per treatment group. Gene expression by qRT-PCR.

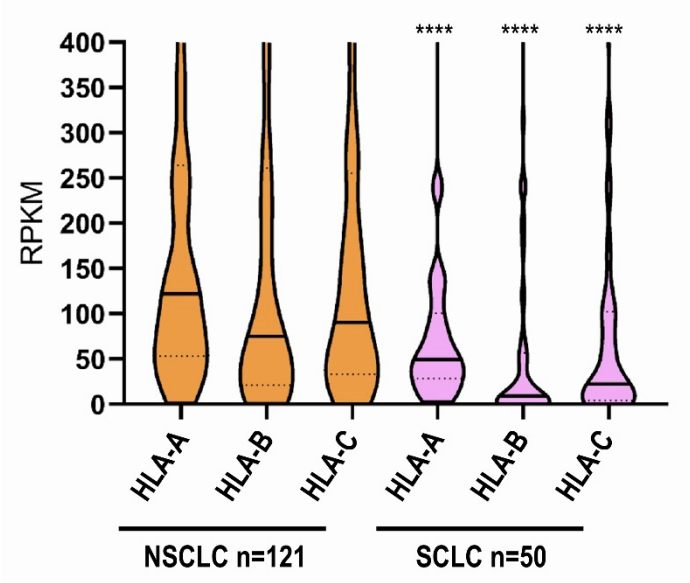

Figure S8 (related to Figure 5). Human NSCLCs express 2-fold or higher levels of MHC Class I molecules than human SCLCs. RNA-sequencing gene expression data from the Cancer Cell Line Encyclopedia, human NSCLC cell lines (n=121) and SCLC cell lines (n=50). Horizontal bar = median, horizontal dash, quartiles. ****p < 0.0001 vs NSCLC. 2-sided Mann-Whitney test.

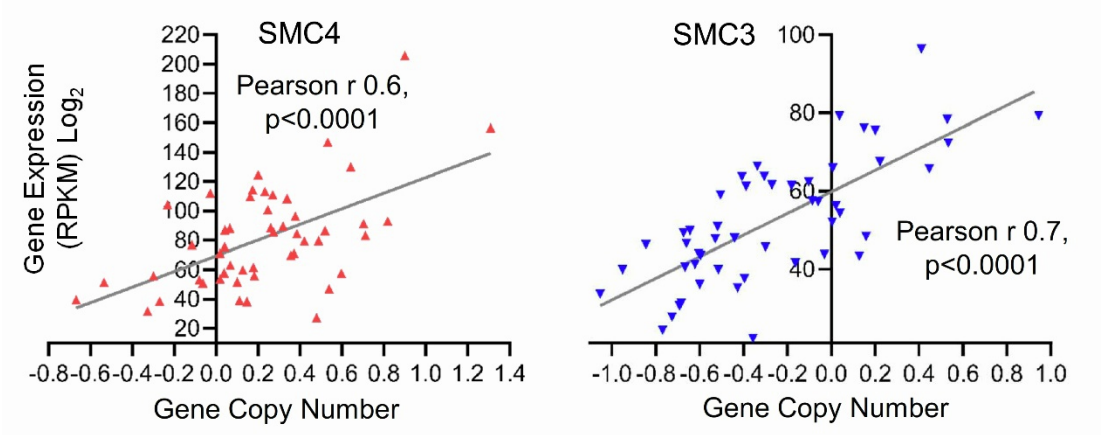

Figure S9 (related to Figure 6, 7). Recurrent amplifications of *SMC4*, with corresponding increases in expression, and recurrent deletions of *SMC3*, with corresponding lower gene expression in SCLC cells. Gene expression by RNA-seq (RPKM, Log2); Normalized copy number (CN) log2 ratios (log2(CN/2) segmented by the circular binary segmentation algorithm, with values <-0.15 considered as deletion and >0.15 as amplification (Cancer Cell Line Encyclopedia, SCLC cell lines n=50)[7].

References

1. Mahadevan, N.R., Knelson, E.H., Wolff, J.O., Vajdi, A., Saigi, M., Campisi, M., Hong, D., Thai, T.C., Piel, B., Han, S., et al. (2021). Intrinsic Immunogenicity of Small Cell Lung Carcinoma Revealed by Its Cellular Plasticity. Cancer Discov *11*, 1952-1969. 10.1158/2159-8290.CD-20-0913.

2. Travaglini, K.J., Nabhan, A.N., Penland, L., Sinha, R., Gillich, A., Sit, R.V., Chang, S., Conley, S.D., Mori, Y., Seita, J., et al. (2020). A molecular cell atlas of the human lung from single-cell RNA sequencing. Nature *587*, 619-625. 10.1038/s41586-020-2922-4.

3. Gehart, H., van Es, J.H., Hamer, K., Beumer, J., Kretzschmar, K., Dekkers, J.F., Rios, A., and Clevers, H. (2019). Identification of Enteroendocrine Regulators by Real-Time Single-Cell Differentiation Mapping. Cell *176*, 1158-1173 e1116. 10.1016/j.cell.2018.12.029.

4. Nazor, K.L., Altun, G., Lynch, C., Tran, H., Harness, J.V., Slavin, I., Garitaonandia, I., Muller, F.J., Wang, Y.C., Boscolo, F.S., et al. (2012). Recurrent variations in DNA methylation in human pluripotent stem cells and their differentiated derivatives. Cell stem cell *10*, 620-634. 10.1016/j.stem.2012.02.013.

5. Mohammad, H.P., Smitheman, K.N., Kamat, C.D., Soong, D., Federowicz, K.E., Van Aller, G.S., Schneck, J.L., Carson, J.D., Liu, Y., Butticello, M., et al. (2015). A DNA Hypomethylation Signature Predicts Antitumor Activity of LSD1 Inhibitors in SCLC. Cancer cell *28*, 57-69. 10.1016/j.ccell.2015.06.002.

6. Nusinow, D.P., Szpyt, J., Ghandi, M., Rose, C.M., McDonald, E.R., 3rd, Kalocsay, M., Jane-Valbuena, J., Gelfand, E., Schweppe, D.K., Jedrychowski, M., et al. (2020). Quantitative Proteomics of the Cancer Cell Line Encyclopedia. Cell *180*, 387-402 e316. 10.1016/j.cell.2019.12.023.

7. Ghandi, M., Huang, F.W., Jane-Valbuena, J., Kryukov, G.V., Lo, C.C., McDonald, E.R., 3rd, Barretina, J., Gelfand, E.T., Bielski, C.M., Li, H., et al. (2019). Next-generation characterization of the Cancer Cell Line Encyclopedia. Nature *569*, 503-508. 10.1038/s41586-019-1186-3.